

Spiral Antenna for UWB RADAR on MF - HF

Antena Espiral de UWB para RADAR en bandas MF y HF

Marlon Patiño-Bernal¹, José David Cely²

Abstract

The ionospheric layer's height and density are measured by the reflected and captured RADAR signals. A vertical incidence pulsed ionospheric RADAR (VIPIR) operates from 1 MHz to 20 MHz. Due to the characteristics of power and directivity, the VIPIR transmitting antennas currently used are large and require up to 30 m height for installation, which is expensive and requires complex assemblies due to their technical complements such as towers, ground systems, and lightning rods. The VIPIR UD system is an ionosonde design with the RADAR signal transmission antenna to be installed near the ground level to reduce investment and complements. The design of the antenna array is assumed from the requirements of frequency range, location, gain, power management, and directivity, a spiral dipole design with a ground plane above the ground is selected, for the analysis of the antenna array on MATLAB, and the optimization process was made with the Antenna Toolbox with the SADEA optimization tool. The results show that the proposed system works according to the requirements, exceeding the directivity by up to 6 dBi in 90% of the target band and 9 dBi on some ranges, resulting in a design that facilitates the assembly of the radar with less structure and height resulting in the reduction of the assembly, operation and subsequent maintenance budget.

¹ Electronic engineer, Universidad Distrital FJDC, Colombia. MSc on telecommunication engineering, Universidad Nacional de Colombia, Profesor asistente Universidad Distrital FJDC marlonpb@udistrital.edu.co ORCID: <https://orcid.org/0000-0002-2363-8731>

² Electronic engineer, Universidad Distrital FJDC, Colombia. Profesor asistente Universidad Distrital FJDC. jdcely@udistrital.edu.co ORCID:<https://orcid.org/0000-0001-8969-5301>

Keywords: Antenna, Antenna array, Electromagnetic analysis, Ionosphere, Optimization, RADAR.

Resumen

La altura y la densidad de las capas ionosféricas se miden mediante señales de radar reflejadas y capturadas. Un RADAR ionosférico pulsado de incidencia vertical (VIPIR) opera desde 1 MHz hasta 20 MHz. Debido a las características de potencia y directividad, las antenas transmisoras VIPIR que se utilizan actualmente son grandes y requieren una instalación elevada de hasta 30 m, lo cual es costoso y requiere montajes complejos debido a sus complementos técnicos como torres, sistemas de tierra y pararrayos. El sistema VIPIR UD es un diseño de ionosonda con la antena de transmisión de señal RADAR que se instalará cerca del nivel del suelo para reducir la inversión y los complementos. El diseño del conjunto de antenas se asume a partir de los requisitos de rango de frecuencia, ubicación, ganancia, administración de potencia y directividad, se escogió un diseño de dipolo en espiral con un plano de tierra sobre el suelo, para el análisis del conjunto de antenas se usa MATLAB, y el proceso de optimización se realizó con el Antenna Toolbox y con la herramienta de optimización "Surrogate Assisted Differential Evolution Algorithm" (SADEA). Los resultados muestran que el sistema propuesto funciona de acuerdo con los requerimientos superando la directividad hasta en 6 dBi en el 90% de la banda objetivo y 9 dBi en algunos rangos, dando como resultado un diseño que facilita el montaje del radar con menor estructura y altura, además de la reducción del presupuesto de montaje, operación y posterior mantenimiento.

Palabras clave: Antena, Arreglos de Antenas, Ionosfera, Optimización, RADAR.

1. Introduction

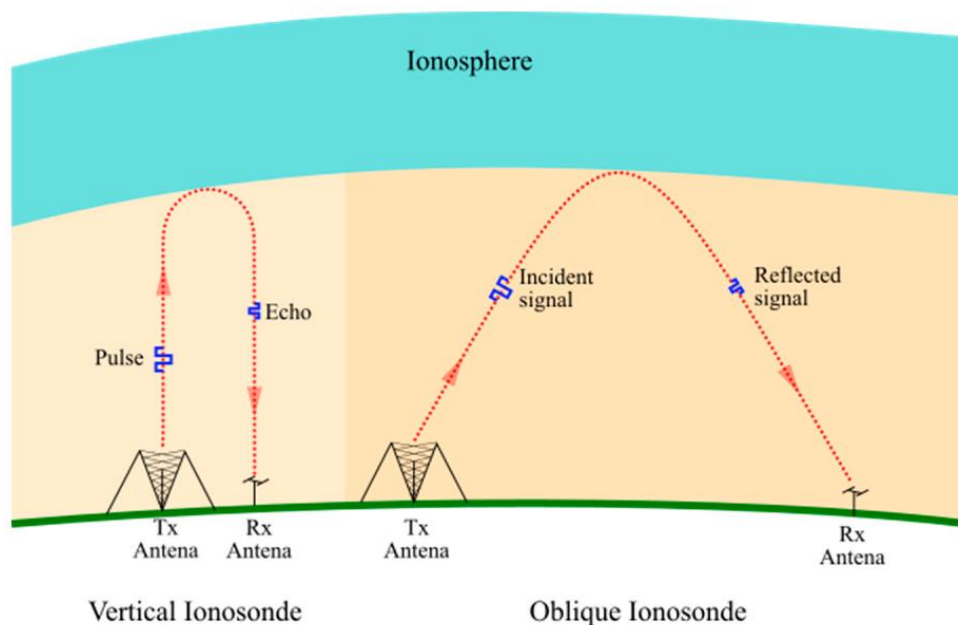
Radar systems for ionospheric measurements operate in sweeps from 500 kHz to 25 MHz, as these signals occupying the MF and HF bands can cause interference to AM broadcast and other services, the range is reduced excluding AM band till 1600 kHz and up to 20 MHz, this limit the interference and reduce size requirements, this range is close to 200% of the central frequency, 10 MHz, so this categorized this rf emission as ultra-wide-band (UWB). The VIPIR emits pulsed signals in a frequency sweep of the entire range and a direction perpendicular to the ground plane [1], [2] Since multiple radiocommunication services operate in the same frequency range, the emission must be directed toward the sky, limiting possible interference with other services and users around the transmission point.

Ionosphere measurements serve scientific and technological purposes, among which we can mention the reduction of the uncertainty of the delay in GPS signals, significantly increasing their accuracy and generating evident improvements in augmented reality applications, and commercial services that complement mobile communications [3], [4].

The simplest ionospheric RADAR system to implement is the Pulsed Signal of Vertical Incidence known as VIPIR as the example in Figure 1, it is also possible to receive VIPIR signals at points far from the transmission site, but this functionality is after the installation of the VIPIR and is not of current interest for this project by the multiple deployment places cost. The VIPIR system uses two separate arrays, one for transmitting and one for receiving, with the lowest-height, lowest-cost receiving arrangement usually consists of a Radar system operating in the ranges of 500 kHz to 25 MHz or more in some cases[5], [6], occupying the MF and HF bands. They emit pulsed signals in a frequency sweep of the entire range and a direction perpendicular to the ground plane[1]. Since there are multiple radiocommunication

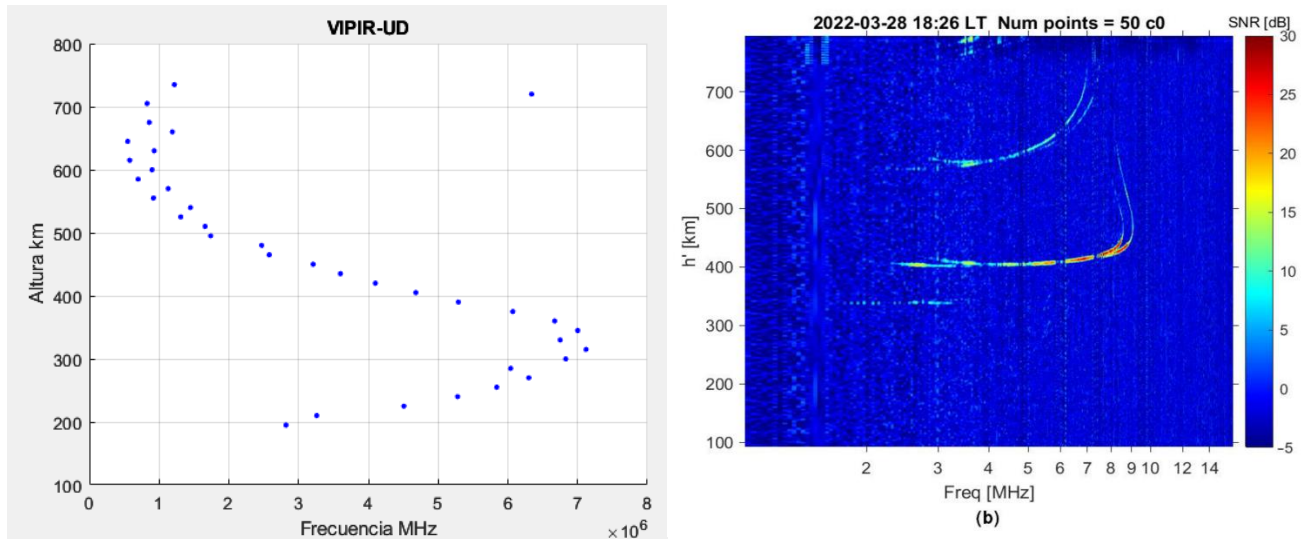
services in the same frequency range,[2] the emission must have a directivity toward the sky that limits possible interference with other services and users around the transmission point.

Figure 1. Ionospheric RADAR or ionosondes. [7]



The wavelengths, which are directly related to the size of the antenna, vary from 600 m to 12 m, with a typical VIPIR assembly with periodic logarithmic arrays LPDA up to 100 m high being typical for high-level and inversion systems or in more limited cases, delta-type antennas of about 30 m high and 60 m wide [1], [8], [9]. These dimensions imply great complexity in assembly and high costs in the transmission system alone, in addition to involving other costs and associated risks, such as greater vulnerability to atmospheric discharges. The main interest of this work is to reduce the size of the VIPIR UD array of transmission antennas and, consequently, the cost of an ionospheric RADAR deployment in Colombia.

Figure 2. Ionogram by Vertical RADAR left is a MATLAB Simulation, right, measurement by Ionosonde from [10].



Source: own.

2. Methodology

The design was chosen based on the analysis of requirements and the possibility of adjusting the height of the arrangement above the ground to respond to HF signals, many array forms were considered and some of them still are in simplifying the optimization process. The main idea was to use a dipole array in a horizontal deployment with which a lower height can be obtained; however, the required area is still very large for the proposed objective because the wavelength for the lower limit of the design exceeds 300 m.

Antenna synthesis and design optimization using evolutionary algorithms (EAs) have been widely applied.[11], [12], [13]. Because antenna synthesis often deals with multimodal black-box optimization problems, it is part of the broader field of evolutionary computation (EC) methods. Other works and research try differential evolution (DE) [12], and particle swarm optimization (PSO) [11] representing two most popular algorithms in antenna synthesis,

Electromagnetic (EM) simulation is often a must in antenna synthesis, and the time needed to perform an EM simulation for a candidate solution varies from a few seconds to tens of minutes [14], or even several hours

The SADEA Algorithm's key idea is to investigate and improve the cooperation between surrogate modeling and EA. Most available Structured Adaptive Evolutionary Algorithms (SAEAs) are based on standard Evolutionary Algorithms (EAs), which require complex modifications in the selection process. The newly generated candidates may be distributed across various areas of the search space to ensure reliable replacements in various subregions, an accurate surrogate model is necessary for different types of data. This goal is achieved using the most accurate function evaluations, which serve as training data or are used for comparison and replacement. In contrast, the SADEA algorithm proposes a new search mechanism that is aware of surrogate models, working in collaboration with a simplified GP model.

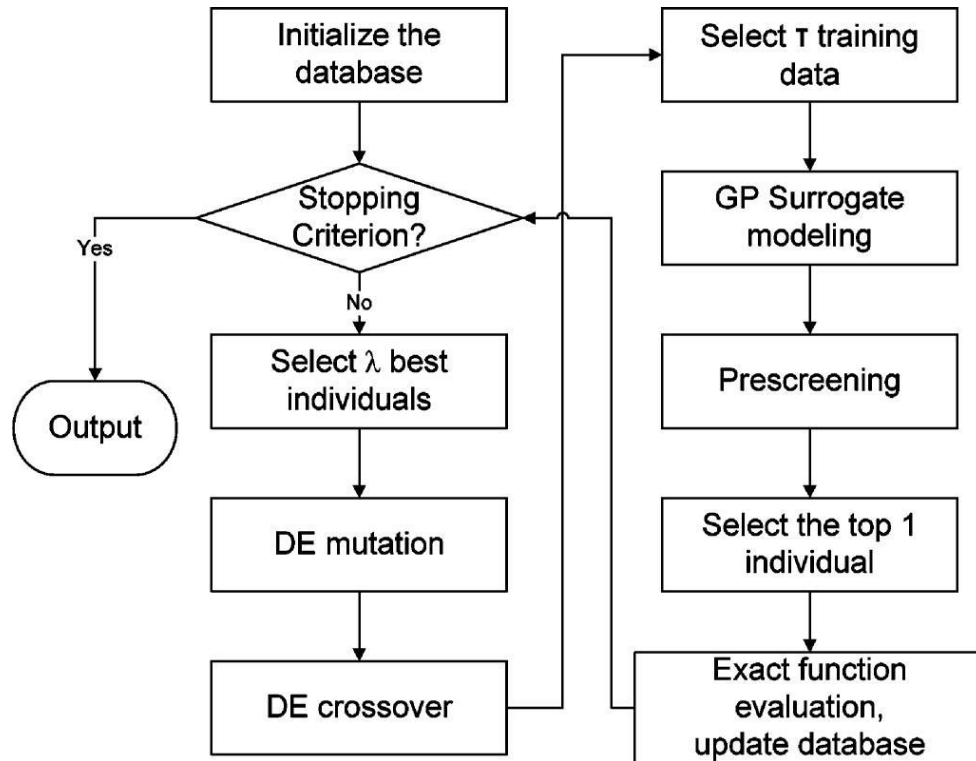
2.1. SADEA Algorithm Outline

The success of SADEA is significantly influenced by the quality of its surrogate model, also an important factor in achieving a good quality of the surrogate model is the number of training data. By more training data is needed for medium- and high-dimensional problems to create a reasonably good surrogate model. As dimensionality increases, the amount of required training data also rises. Although only a limited amount of training data is used, the above special surrogate model can be achieved if the training data are near the top-ranked candidates in the group of newly generated candidates, the SADEA outline and steps were proposed on [15]

2.1.1. Initialization.

The database initialization utilizes a Design of Experiments (DOE) method for optimization known as Latin Hypercube sampling (LHS), this is used to generate α design samples from initial value ranges $[a,b]$, evaluate all the design samples using EM simulations and then use them to form the initial database. $[a,b]$ This is the search range defined by the user. The value of α is determined self-adaptively.[16]. The LHS sampling method samples the design space more uniformly, and hence, needs fewer samples to achieve more effective sampling.

Figure 3. SADEA Flow Diagram from [15]



2.1.2. Iteration steps.

- Choose the λ best candidate designs from the database to create a population P . Revise the best candidate design we have developed so far, so the value of λ is determined self-adaptively. Use the current-to-best mutation method in differential evolution. and binomial crossover operators on P to generate λ child solutions, for each child solution

in P , select τ nearest design samples based on Euclidean distance as the training data points and construct a local Gaussian process surrogate model. The value of τ is determined adaptively

- Prescreen the λ child solutions generated before by using the Gaussian process surrogate model with the lower confidence bound prescreening.
- Perform an EM simulation on the best-prescreened child solution and add this simulated candidate design along with its function value to the database.

2.1.3. Stopping criteria

- The specification goal is met.
- The standard deviation of the population is smaller than the threshold.
- The computing budget for EM simulations has been exhausted. Additional EM simulations can be added at any time.

3. Reduced Siza VIPIR antenna

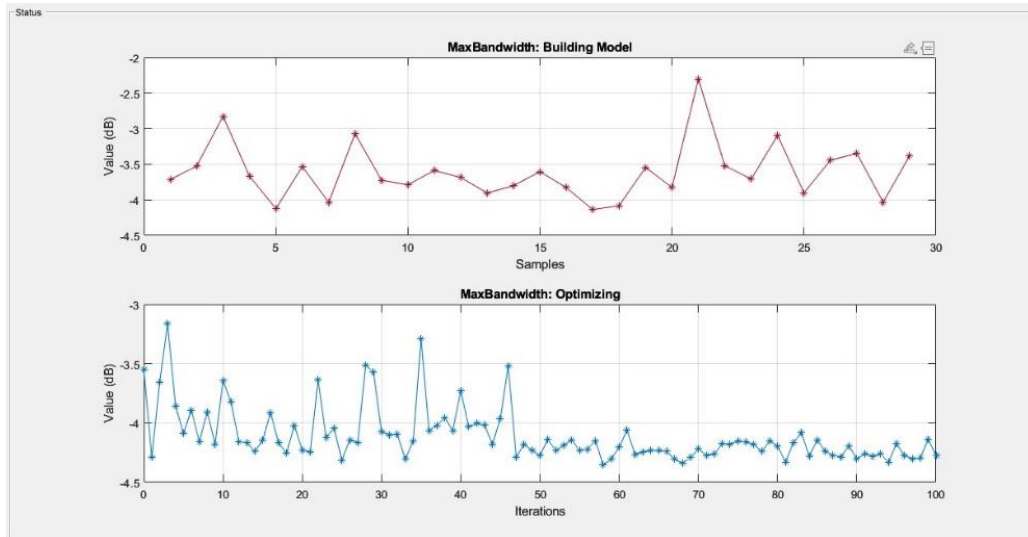
For this work, a spiral dipole with a ground plane that also acts as a reflector was selected, Figure 4, the spiral dipole has an adequate electrical longitude and the wide of the spiral can adjust a good impedance match for the entire range from 2 MHz to 20 MHz.

An iterative optimization process [17] was used which led to the design shown in this work after evaluating 100 processes where physical variables such as height and geometric variables such as the separation of the spirals and the width of these spirals were adjusted.

The variables to be optimized were bandwidth and array gain. Although in advance the array assumes low directivity in the lower frequencies of 2 MHz with gains close to 3dBi and a significant improvement in the high 20 MHz being viable to expect values close to 12 dBi.

The resulting values were reached after interaction 47, as can be seen in Figure 3 with subsequent results up to 100 being very similar, although it is not possible to rule out models with better performance values such improvements are not expected to be of importance.

Figure 4. SADEA optimization process numbers, performed in MATALAB.

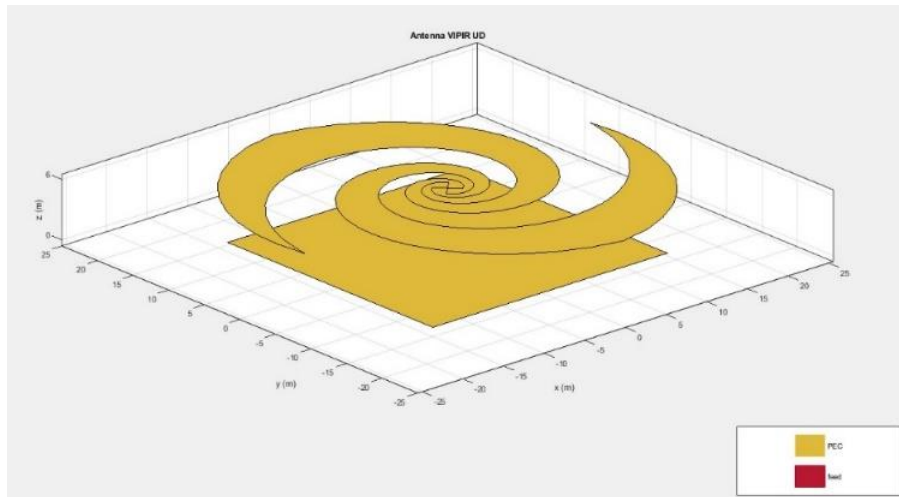


Source: own.

4. Spiral antenna and a reduced ground plane for VIPIR results

From the optimization process, the wide, longitude and other characteristics of the spiral antenna were modified to find the best bandwidth and gain. Since the height of the antenna above the ground plane is related to the gain and directivity in special on lower frequencies, the optimization process always sets the height at the maximum of the available range. In this case 5 m, the spiral design reaches a square of 20 m by 20 m and the spiral arms reach 45 m each one, the general aspect of the design can be seen in Figure 5.

Figure 5. Spiral antenna design for VIVPIR UD obtained on MATLAB.

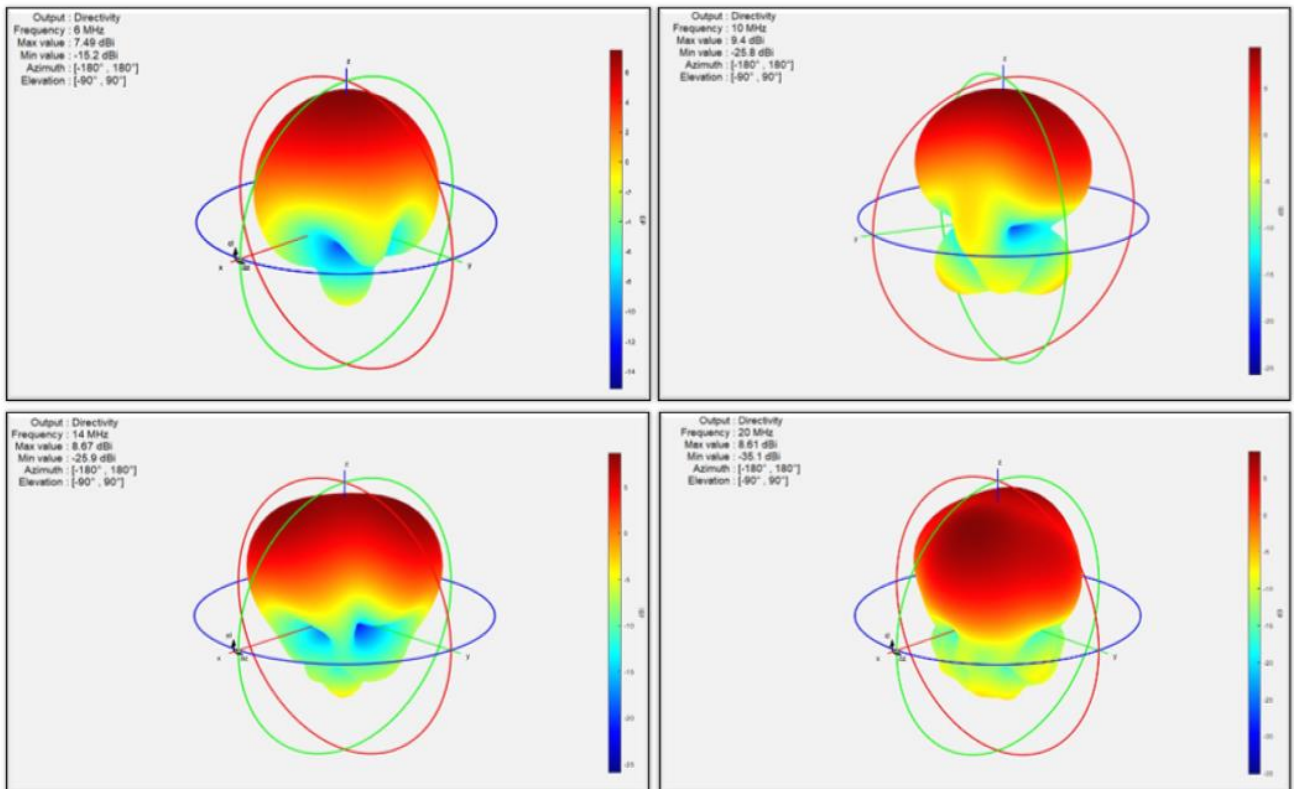


Source: own.

The gain of the design varies from 5 dBi on the lower frequencies 2MHz to 9 dBi at 20 MHz.

Clarifying that in the lower frequencies, the front-to-back ratio is 3dB. A radiation pattern set can be seen in Figure 6.

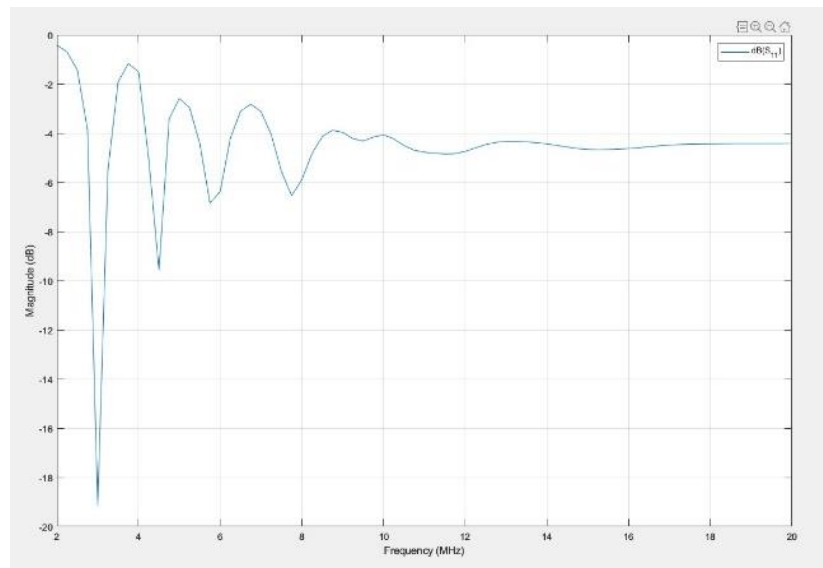
Figure 6. Gain and radiation pattern on 6 MHz of the VIVPIR UD array.



Source: own.

The scattered parameter S11 or reflection parameter behavior can analyze on Figure 6. The design shows performance from 2MHz to 20 MHz, the better the behavior the larger the magnitude of the absorption on dB.

Figure 7. Scattered parameter S11 Vs frequency of the designed VIPIR array on MATLAB.



Source: own.

5. Discussion

The obtained antenna design does not effectively cover the entire proposed range, at low frequencies due to the dimensions of the design with wavelength. Although it can operate from 2 MHz its most useful operation is from 3 MHz and can be extended to the entire HF band from 3 to 30 MHz. It was clear from the design that the greater the separation from the ground plane, the better its operation would be in the lower part of the range.[18]

Current and upcoming work with the design proposes ways to improve gain at low frequencies by adding capacitive or inductive loads to extend the electrical length of the spiral arms What can be achieved with variations in the width of each arm but with the implications of the effect of these loads on the higher frequencies. We are also working on the possibility of using a

design for the range of 1 MHz to 5 MHz that complements the one presented here that works very well from 3 to 20 MHz.

The design presented represents a feasible option for the mounting of the ionospheric RADAR VIPIR UD with an infrastructure of lower height above the ground and with operational characteristics like the antenna system traditionally used as a delta antenna for VIPIR systems. This antenna design results in an innovation for the subject because so far in reviews on the subject we have not had similar proposals in form or performance.

SADEA is an artificial intelligence (AI) tool designed to enhance antenna design methods. It is based on machine learning and evolutionary computation techniques. This approach offers several advantages, including improved optimization quality, greater efficiency, enhanced generality, and increased robustness. SADEA algorithm carries out global optimization and employs a surrogate model built by statistical learning techniques. The method to make surrogate modeling and optimization work harmoniously is critical in such surrogate model-assisted optimization methods. In SADEA, some ideas of the surrogate model-aware evolutionary search framework are borrowed, see [3] and [4]. SADEA uses differential evolution (DE) as the search engine and Gaussian process (GP) machine learning as the surrogate modeling method applied as AI mechanism to optimize EM design, devices, and conditions, has been developed, and SADEA, as the multi-objective tool is suitable for the synthesis of RADAR antennas.

6. References

- [1] T. Bullett, R. Livingston, R. Grubb, N. Zabotin, "High Frequency Radars and Ionospheric Sounding with VIPIR", 2020.
http://lisn.igp.gob.pe/files/first_ionosonde_school/bullet_HF_sounding.pdf
- [2] T. Bullett, "Dynasonde and VIPIR Ionosonde Field Site Requirements Basic and Research Capabilities", 2018.
ftp://ftp.ngdc.noaa.gov/ionosonde/documentation/VIPIR/VIPIR_Site_Needs-Sep18.pdf

- [3] T. R. Robinson, "Some analytical results for the propagation and spreading of short electromagnetic pulses in the ionosphere," in IEE Colloquium on Antenna and Propagation Problems of Ultrawideband Radar, pp. 10/1-10/5, 1993.
- [4] C. Wang, M. Zhang, Z. Xu, and C. Chen, "Simulation of ionospheric effects on SAR imaging with noise at P-band," in ISAPE2012, 2012, pp. 419-422. <https://doi.org/10.1109/ISAPE.2012.6408795>
- [5] E. Zuccheretti, "Ionospheric radars development," 2010. <https://www.earth-prints.org/bitstream/2122/6958/1/Posgrado.pdf>
- [6] T. W. Bullett, N. A. Zabotin, R. C. Livingston, R. N. Grubb, J. E. Mabie, and C. Negrea, "HF radar measurements of the ionosphere using dynasonde methods", in 2014 XXXIth URSI General Assembly and Scientific Symposium (URSI GASS), 2014. <https://doi.org/10.1109/URSIGASS.2014.6929845>
- [7] J. Talukdar, B. Mehta, K. Aggrawal, and M. Kamani, "Implementation of SNR estimation based energy detection on USRP and GNU radio for cognitive radio networks," in 2017 International Conference on Wireless Communications, Signal Processing and Networking (WiSPNET), 2017, pp. 304-308. <https://doi.org/10.1109/WiSPNET.2017.8299767>
- [8] M. Floer, "Design and Implementation of a Software Defined Ionosonde", 2020. <https://munin.uit.no/handle/10037/19423>
- [9] B. Isham, "An MF/HF antenna array for ionospheric sounding and measurement of ionospheric radio emissions," in 2013 US National Committee of URSI National Radio Science Meeting (USNC-URSI NRSM), 2013. <https://doi.org/10.1109/USNC-URSI-NRSM.2013.6525062>
- [10] O. Koloskov, A. Kashcheyev, O. Bogomaz, A. Sopin, B. Gavrylyuk, and A. Zalizovski, "Performance Analysis of a Portable Low-Cost SDR-Based Ionosonde," Atmosphere (Basel), vol. 14, no. 1, p. 159, Jan. 2023. <https://doi.org/10.3390/atmos14010159>
- [11] Q. Bai, "Analysis of the particle swarm optimization algorithm", Computer and Information Science, vol. 3, no. 1, 2010. <https://doi.org/10.5539/cis.v3n1p180>
- [12] P. Rocca, G. Oliveri, and A. Massa, "Differential evolution as applied to electromagnetics," IEEE Antennas Propag Mag, vol. 53, no. 1, 2011. <https://doi.org/10.1109/MAP.2011.5773566>
- [13] A. Hoorfar, "Evolutionary programming in electromagnetic optimization: A review", IEEE Transactions on Antennas and Propagation, vol. 55, no. 3, 2007. <https://doi.org/10.1109/TAP.2007.891306>
- [14] M. John, M. J. Ammann, "Antenna optimization with a computationally efficient multiobjective evolutionary algorithm," IEEE Trans Antennas Propag, vol. 57, no. 1, 2009. <https://doi.org/10.1109/TAP.2008.2009775>
- [15] B. Liu, A. Irvine, M. O. Akinsolu, O. Arabi, V. Grout, and N. Ali, "GUI design exploration software for microwave antennas," J Comput Des Eng, vol. 4, no. 4, 2017. <https://doi.org/10.1016/j.jcde.2017.04.001>

- [16] M. Stein, "Large sample properties of simulations using latin hypercube sampling," *Technometrics*, vol. 29, no. 2, 1987. <https://doi.org/10.1080/00401706.1987.10488205>
- [17] B. Liu, H. Aliakbarian, Z. Ma, G. A. Vandenbosch, G. Gielen, "An efficient method for antenna design optimization based on evolutionary computation and machine learning techniques," *IEEE Trans Antennas Propag*, vol. 62, no. 1, 2014. <https://doi.org/10.1109/TAP.2013.2283605>
- [18] Z. Ma, G. A. Vandenbosch, "Low-cost wideband microstrip arrays with high aperture efficiency," *IEEE Trans Antennas Propag*, vol. 60, no. 6, 2012. <https://doi.org/10.1109/TAP.2012.2194685>